THE JOURNAL OF PHYSICAL CHEMISTRY B

ARTICLE

pubs.acs.org/JPCB

Determination of Physicochemical Parameters of Ionic Liquids and Their Mixtures with Solvents Using Laser-Induced Gratings

Dimitrii N. Kozlov,[†] Johannes Kiefer,[*,§,∥] Thomas Seeger,[‡,§,⊥] Andreas P. Fröba,[‡,§] and Alfred Leipertz[‡,§]

[†]A.M. Prokhorov General Physics Institute, Russian Academy of Sciences, 119991 Moscow, Russia

[‡]Lehrstuhl für Technische Thermodynamik (LTT), Universität Erlangen-Nürnberg, D-91058 Erlangen, Germany

[§]Erlangen Graduate School in Advanced Optical Technologies (SAOT), D-91058 Erlangen, Germany

[∥]School of Engineering, University of Aberdeen, Aberdeen AB24 3UE, Scotland, U.K.

[⊥]Lehrstuhl für Technische Thermodynamik, Universität Siegen, D-57076 Siegen, Germany

ABSTRACT: The laser-induced gratings (LIGs) technique has been applied for the simultaneous determination of sound speed and thermal diffusivity in the room temperature ionic liquid (RTIL) 1-ethyl-3-methylimidazolium ethylsulfate, [EMIm][$EtSO_4$], its mixture with 85.68 mol % acetone, C_3H_6O, and pure acetone. The measurements have been performed in a quartz glass cuvette at ambient pressure and temperature. Radiation of a pulse-repetitive Q-switched Nd:YAG pump laser (1064 nm) effected quasi-resonant excitation of overtone-combinational vibrational states of the RTIL molecules followed by the appearance of laser-induced gratings. The temporal evolution of the transient gratings (oscillation and damping) was recorded using Bragg-diffraction of a continuous-wave probe laser radiation. From the LIG signals' temporal profiles, values of the sound speed and thermal diffusivity were determined and, in addition, the isentropic compressibility and thermal conductivity were derived. The results are in a reasonable agreement with those reported in the literature. Furthermore, since the data for the determination of the physicochemical properties can be obtained with a single laser pulse, the LIG technique has potential for applications where data acquisition at high repetition rates is desirable for example to monitor processes.

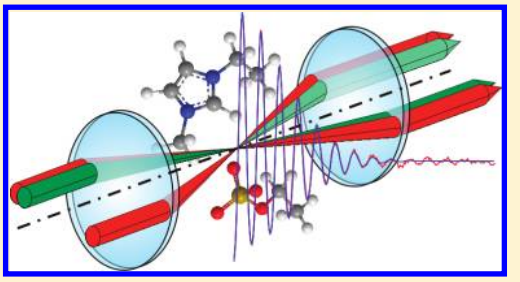

1. INTRODUCTION

Room-temperature ionic liquids (RTILs) have been found to have beneficial properties for a wide range of applications, for example, as solvents, reaction media, and electrolytes.[1] These properties are existing over wide temperature ranges and often include high-dissolving power, extremely low or even negligible vapor pressure, nonflammability, and high electroconductivity combined with good thermal and electrical stability.[1−4] As a consequence, over the past two decades RTILs have attracted an increasing interest from academia as well as industry. A major aim of the studies is to investigate and understand the relations between molecular structure and macroscopic properties of RTILs and their mixtures with other solvents. Owing to the huge number of potential combinations of cations and anions composing RTILs, this profound understanding will allow tailor-making of fluids for specific applications in the future. Such applications may include catalytic processes and biotransformations,[5] separation technology,[6] and the use as electrolytes.[7]

In order to reach this understanding of the fundamental properties of RTILs and hence of their applicability for practical tasks, a large variety of approaches, both theoretical and experimental ones, has been and is being employed for studying pure liquids and their mixtures with cosolvents. The aim is to get the data that would provide possibilities to predict the desired properties of a liquid at a given composition and temperature in order to avoid the need for excessive measurements. For fundamental analysis of molecular structure and intermolecular interactions, various spectroscopic techniques have been very successful, often in combination with theoretical methods based on ab initio or density functional theory calculations (see, for example, recent results from our group[8]). From a practical viewpoint, however, the macroscopic properties of RTILs and their mixtures are of interest. Hence, a wide range of conventional methods,[1−4] as well as light scattering techniques,[9] have been employed to measure their physicochemical properties.

One attractive method to study RTILs is the nonlinear optical technique employing laser-induced gratings (LIGs, also known as transient gratings, TGs), that is, locally excited spatially periodic modulations of the refractive index.[10] It enables the noncontact determination of multiple parameters, including speed of sound, thermal diffusivity, and acoustic damping rate, in a single measurement. In a typical LIG experiment, two pump beams from a pulsed laser are coherently overlapped to generate an interference pattern in the intersection region. Electrostriction and/or redistribution of the excessive internal energy of molecules excited by pump radiation lead to a transient density and,

Received: April 19, 2011
Revised: May 27, 2011
Published: May 31, 2011

hence, refractive index spatial modulation. The evolution of the transient grating can be recorded by detecting the power of Bragg-diffracted radiation of a third, continuous-wave probe laser beam with high temporal resolution. Eventually, from this signal information about the local properties of the medium can be extracted. An important feature of the LIGs technique is that it delivers data on a single-shot basis. Hence, it can provide measurements at high rate (determined by the repetition rate of the pump laser, which is typically in the order of tens of hertz). This makes LIGs a potential method for real-time process monitoring. Details of the technique can be found in ref 10 and its application for studying thermal diffusivity in liquids was described, for example, in ref 11.

A few studies employing the LIGs technique to investigate RTILs have been presented recently. In ref 12, combinations of the cation 1-butyl-3-methylimidazolium ([BMIm]) with different anions, and combinations of the anion bis(trifluoromethylsulfonyl)imide ([Tf_2N]) with different cations have been studied to determine the effect of anion and cation on the thermophysical properties of the RTILs. Within the approach employed in ref 12, measurements were carried out using ionic liquids with small concentrations of an inert ferroin dye that was excited by the 532 nm output of a Nd:YAG laser to create LIGs due to thermalization of the absorbed energy. In ref 13, the transport and equilibrium properties of binary mixtures of CO_2 and 1-butyl-3-methylimidazolium hexafluorophosphate ([BMIm][PF_6]), like thermal diffusivity, sound speed, and thermal conductivity, have been investigated at room temperature in dependence on CO_2 pressure. For this purpose, the exothermic photodissociation reaction of diphenylcyclopropenone, admixed to the RTIL, has been initiated in a spatially periodic way by the 355 nm output of a Nd:YAG laser to generate LIGs. The mentioned experiments have in common that laser-induced gratings have been created through excitation of molecules added to the RTIL under investigation.

In the present work, we accomplish the generation of LIGs directly in the ionic liquid 1-ethyl-3-methylimidazolium ethylsulfate ([EMIm][$EtSO_4$]) and its binary mixture with the organic solvent acetone, C_3H_6O, so that no additives such as dye molecules need to be used. Molecular structures of the [EMIm] cation, the [$EtSO_4$] anion, and acetone are shown in Figure 1. The RTIL under study attracts particular interest since it is one of the first that has been synthesized on technical scale and is commercially available from almost all major chemical suppliers. Its spectroscopy and structure has been investigated using Raman scattering and infrared absorption,[14] as well as density functional methods.[15] In the present work, we make use of the weak vibrational overtone-combinational absorption bands of [EMIm][$EtSO_4$] in the near-infrared region around 1000 nm and accomplish excitation of LIGs by employing the 1064 nm output of a pulsed Nd:YAG laser. This approach is demonstrated to be appropriate for the measurements of sound speed and thermal diffusivity in the pure [EMIm][$EtSO_4$] and C_3H_6O, as well as in their binary mixtures. Furthermore, isentropic compressibility and thermal conductivity are determined. The values obtained for the pure samples are compared with those available in the literature.

2. EXPERIMENTAL SECTION

2.1. Experimental Setup. The experimental setup used for generating laser-induced gratings and recording the temporal evolution of the LIG signals has been described in detail in ref 16

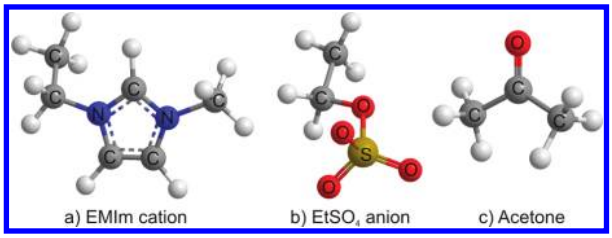

Figure 1. Molecular structures of the [EMIm] cation, the [$EtSO_4$] anion, and acetone.

and is schematically similar to those from refs 12 and 13. Briefly, a linearly polarized, Q-switched pulse-repetitive Nd:YAG laser (7 ns, 10 Hz, λ_p = 1064 nm) has been used as the pump laser. It provided two pump beams with parallel polarization and pulse energies attenuated to be about 0.6 mJ each. Radiation of a frequency-doubled cw Nd:YAG laser (λ = 532 nm, 17 mW) has been employed as a probe. The three collinear beams were focused into the probe volume (about 400 μm diameter) by a f = 1000 mm lens where they crossed at the appropriate phase matching angles. The crossing angle of the pump beams ($\theta_p \approx 2.1°$) was providing the fringe spacing $\Lambda = \lambda_p/2 \sin(\theta_p/2) \approx 29.0\ \mu$m. The probe radiation was Bragg diffracted by the gratings that enabled to observe their temporal evolution. The diffracted radiation was recollimated by the second lens and then was passed through an interference filter and an optical fiber, transferring the light to a photomultiplier tube. The PMT output was directed to a 3 GHz bandwidth digital oscilloscope connected to a computer, which accomplished time-resolved recording of the diffracted light intensity variation corresponding to the temporal evolution of a LIG. The liquid samples filled in quartz glass cuvettes of 10 mm thickness were placed into the intersection area of the beams. The temperature of the samples was assumed to be identical with the room temperature of about 293 K.

2.2. Sample Preparation and Spectroscopic Characterization. In this work, samples of pure [EMIm][$EtSO_4$], pure acetone, and their binary mixture (60 mass %, or 85.68 mol % of acetone) have been investigated. Details of [EMIm][$EtSO_4$] synthesis and the sample preparation procedure are given in ref 17.

The RTIL under investigation has been characterized spectroscopically in previous studies. A vibrational study of [EMIm][$EtSO_4$] in the frequency range of 500−3500 cm^{-1} using Raman and FTIR spectroscopy has been reported in ref 14. In a recent work,[15] Raman and IR spectra (300−3800 cm^{-1}) as well as the absorption spectrum (200−1000 nm) have been compared with data obtained from density functional theory calculations to study interionic interactions. For the present work, the absorption spectra in the visible and near-infrared regions are of interest. Therefore, the spectra of [EMIm][$EtSO_4$] and acetone have been recorded between 600 and 2600 nm using a Shimadzu UV-3600 spectrophotometer with a spectral resolution of 2 nm. For the measurements, [EMIm][$EtSO_4$] and C_3H_6O samples were filled into quartz glass cuvettes with defined absorption path lengths of 1 and 10 mm. The latter were used to obtain spectra with reasonable amplitudes of the absorption bands in the spectral range of interest, that is, around 1000 nm (recall that the pump laser operates at λ_p = 1064 nm), where the absorption is extremely weak.

3. RESULTS AND DISCUSSION

3.1. Absorption Spectra. The absorption spectra of [EMIm][$EtSO_4$] and C_3H_6O in the visible-to-NIR range

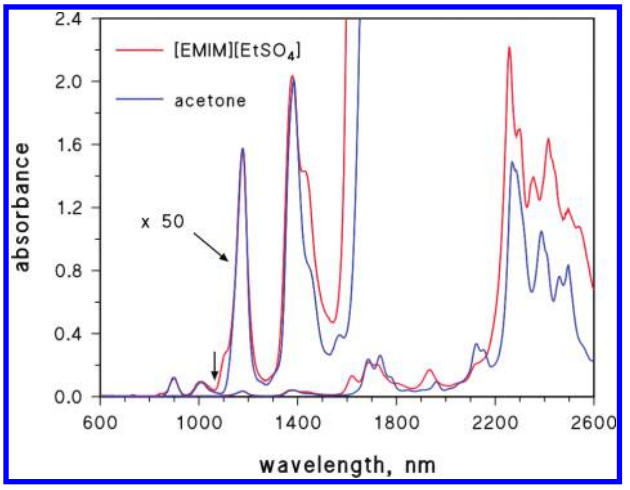

Figure 2. Absorption spectra of [EMIm][$EtSO_4$] and acetone: the general view and the enlarged part in the range of 600−1600 nm; the wavelength of the pump radiation is marked by the vertical arrow.

(600−2600 nm) are displayed in Figure 2. The parts in the range of 600−1600 nm are enlarged to show weak absorption lines. Both spectra look very similar, especially around 1000 nm. This can be explained by the fact that all the major absorption features are related to vibrations in CH_3 groups, which are present in the cation and anion of the RTIL as well as in the acetone molecule (see Figure 1). In particular, the weak absorption lines at 900 and 1010 nm are formed by the transitions to the fourth overtone of the CH bond stretching vibrations and to the overtone-combinational vibrational states containing 3 quanta of these vibrations, respectively. The stronger line at 1180 nm may correspond to their third overtone.

The pump radiation at λ_p = 1064 nm is absorbed with similar efficiency by both the RTIL and acetone at the wing of the 1010 nm absorption line. Despite of the weak absorption ($\alpha \sim 0.015$ cm^{-1}), the small amount of the absorbed and thermalized laser energy is sufficient for generating a reasonably strong LIG signal.

3.2. LIG Signals. *3.2.1. Excitation of Laser-Induced Gratings and Formation of LIG Signals.* The absorption spectra show that both [EMIm][$EtSO_4$] and C_3H_6O molecules experience quasi-resonant excitation by the pump radiation resulting in generation of LIGs. Figure 3 presents an example of a LIG signal recorded in pure [EMIm][$EtSO_4$] at time scales of 0.5 and 500 μs. Qualitatively, the temporal profiles of LIG signals recorded in acetone as well as those obtained in the RTIL/acetone mixture look very similar to that one, and therefore they are not shown. All profiles are characterized by quickly damped high-frequency oscillations at a short time scale and by an exponential decay at a long one.

The characteristic temporal shape of the signal in Figure 3a indicates that the nanosecond-pulse excitation of molecules by 1064 nm radiation within the volume of the fringe pattern is followed by an extremely rapid redistribution of the nonequilibrium vibrational internal energy. This energy redistribution, which can take place either inside the molecules or in the course of resonant energy exchange between the molecules, leads to local temperature variations and hence to modulations of the liquid density. These modulations have the form of a superposition of two acoustic waves that counter-propagate in opposite directions, perpendicular to the planes of the fringes, and a

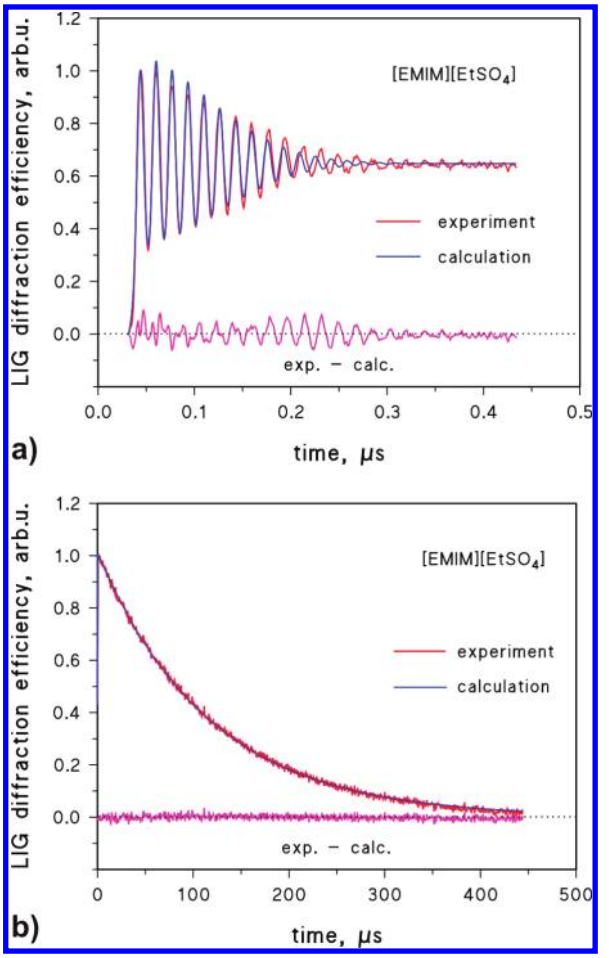

Figure 3. Example of a LIG signal in pure [EMIm][$EtSO_4$]: (a) initial part; (b) large delay part. The result of modeling and the difference between the experimental and calculated values is shown.

slow decaying stationary density grating. With the same amplitudes and the wavelengths equal to the fringe spacing Λ, these waves represent a standing acoustic wave with the oscillation period $T_a = \Lambda/v_s$, where v_s is the adiabatic sound speed within the probe volume. The whole set of these oscillatory and slowly decaying stationary density variations results in the modulations of the refractive index referred to as thermal laser-induced gratings.

Under the same conditions of excitation, electrostriction, the proportional to the square of the electric field strength deformation of dielectric materials in an electric field, produces a spatially periodic adiabatic compression of the medium. As a result, a standing acoustic wave (similar to that provided by rapid energy redistribution) is generated. The corresponding contribution to the modulation of the refractive index is referred to as electrostrictive laser-induced grating.

The diffraction efficiency of LIGs is proportional to the square of the refractive index variation, and it is the evolution of this value that defines the temporal variations of the diffracted light intensity. In particular, the contributions to LIGs caused by the acoustic waves oscillate in time. The corresponding oscillations of the diffracted light intensity are clearly observed in the initial part of the LIG signals recorded in the pure RTIL (see Figure 3a) and in the other samples.

The evolution of LIGs formed by redistribution of the absorbed laser energy depends on the value of the characteristic

time constant τ of this process. "Instantaneous" or "fast" energy redistribution (with $\tau \ll T_a/2\pi$) generates a standing acoustic wave and a stationary density grating. "Slow" energy release (with $\tau \gg T_a/2\pi$) favors the formation of a stationary density grating, while the development of the acoustic contribution is suppressed. In this context, "short laser pulse" means that for the pump laser pulse duration τ_L the condition $\tau_L \ll T_a$ is fulfilled, while the characteristics instantaneous and fast correspond to the cases $\tau \ll \tau_L$ and $\tau \sim \tau_L$, respectively. Specifically, the period T_a corresponding to the oscillations of the LIG signal in pure [EMIm][$EtSO_4$] (Figure 3a) is found to be 17 ns, while it is 25 and 23 ns in pure C_3H_6O and the mixture, respectively.

In our case of focused pump beams, the observed quick damping of the standing acoustic wave amplitude (see Figure 3a) is a result of the divergence of the two counter-propagating acoustic wave packets traveling out of the excitation volume, rather than of significantly slower absorption of sound due to viscosity and heat conduction of the medium. The stationary density modulation slowly decays by heat conduction alone (see Figure 3b).

3.2.2. LIG Signal Evaluation Approach and Derived Parameters. Assuming that part of the energy absorbed by laser-excited species is dissipated instantaneously and the rest of it is further rapidly redistributed during a small finite time τ, and including the electrostrictive contribution, the following approximate relation for the LIG signal strength can be used to describe its temporal evolution and to define its parameters

$$S(t) \cong S_0\left\{M_i\left[\cos \Omega_a t \exp\left(-\left(\frac{t}{\tau_{tr}}\right)^2\right) - \exp\left(-\frac{t}{\tau_{th}}\right)\right] + M_f\left[\left(\frac{k_f}{1+k_f^2}\sin \Omega_a t + \frac{1}{1+k_f^2}\cos \Omega_a t\right)\exp\left(-\left(\frac{t}{\tau_{tr}}\right)^2\right) - \frac{\left[\exp\left(-\frac{t}{\tau_{th}}\right) - \exp\left(-\frac{t}{\tau_f}\right)\right]}{\tau_f\left(\frac{1}{\tau_f} - \frac{1}{\tau_{th}}\right)} - \frac{1}{1+k_f^2}\exp\left(-\frac{t}{\tau_f}\right)\right] + M_e \sin \Omega_a t \exp\left(-\left(-\frac{t}{\tau_{tr}}\right)^2\right)\right\}^2 \quad (1)$$

Here S_0 is a LIG signal scaling factor; M_i, M_f, and M_e are dimensionless coefficients which scale the contributions to LIGs as a result of instantaneous and finite time (fast) energy redistributions, and electrostriction, respectively; the acoustic frequency Ω_a is defined as $\Omega_a = 2\pi/T_a$, τ_f is the characteristic time constant of the fast relaxation process, and $k_f = \Omega_a\tau_f$; the decay of signal oscillations is defined by the acoustic transit time τ_{tr}, which accounts for the movement of the two counter-propagating acoustic wave packets. The stationary density modulation damping constant τ_{th} is related to the thermal diffusivity χ[18]

$$\tau_{th} = \left(\frac{\Lambda}{2\pi}\right)^2 \chi^{-1} \quad (2)$$

which in turn is defined as

$$\chi = \left(\frac{\kappa}{\rho c_P}\right) \quad (3)$$

where κ is the thermal conductivity, ρ is the density, and c_P is the specific heat capacity at constant pressure.

Table 1. Fitted Temporal Parameters and Calculated Values of T_a[a]

	Ω_a, μs^{-1}	T_a, ns	τ_f, ns	τ_{th}, μs	τ_{tr}, μs
[EMIm][$EtSO_4$]	380 ± 2	16.5	3.7	233 ± 2	0.120
C_3H_6O	254 ± 1	24.7	1.3	206 ± 2	0.126
RTIL/C_3H_6O mixture	276 ± 1	22.8	1.3, 3.7	235 ± 2	0.092

[a] The errors are estimated based on the variation of the parameter values derived from independent measurements.

Equation 1 can be obtained using the linearized hydrodynamic equations for the density and temperature variations,[19,20] assuming a two-stage energy redistribution process, and introducing the decay factor $\exp(-t/\tau_{tr})^2)$ for the oscillating contribution. It can be reduced to eq 4 in ref 12 or eq 1 in ref 13 (except the exponential decay of the oscillating term) under further simplifying assumptions that the electrostrictive contribution can be neglected and condition $\tau_f \ll \tau_L$ is fulfilled. In general, the parameters of interest Ω_a and τ_{th} are derived from the experimental data by nonlinear fitting the temporal shape of a LIG signal with the curve defined by eq 1.

The absorption spectra show that both [EMIm][$EtSO_4$] and C_3H_6O molecules are excited by pump radiation. Hence, the excitation of molecules in a mixture is nonspecific. As a consequence, the observed resemblance of LIG signals in pure species and in their mixture might be a result of the similarity of absorbing molecular structure elements and probably of the mechanisms of the nonequilibrium internal energy redistribution.

The LIG signals recorded in [EMIm][$EtSO_4$], C_3H_6O and their mixture have been fitted using eq 1. The results show that taking into account electrostrictive, instantaneous, and fast thermal contributions allows one to reasonably fit the signal temporal profiles (as demonstrated in Figure 3). The difference between the observed and fitted LIG signals for [EMIm][$EtSO_4$] is also shown in Figure 3. Note that the signal oscillations in Figure 3a initially show good agreement between experimental and modeled data but reveal some discrepancy in the oscillation amplitude and phase after 9−10 oscillation periods at delays of 0.170−0.270 μs before they are finally damped out. This may be an experimental artifact due to the alignment of the laser beams. However, the acoustic frequency is basically determined by the strong initial oscillations, and therefore the mentioned deviations at longer delay times do not play a significant role. Similar quality of fitting has been obtained for the other samples. Hence, one can conclude that in our case the following two different mechanisms are responsible for LIGs formation: electrostriction and energy redistribution. This situation of exciting [EMIm][$EtSO_4$] and C_3H_6O to vibrational levels, which are characterized by a finite relaxation time, differs from the excitation of higher-energy electronic states of admixtures in refs 12 and 13, which is accompanied by instantaneous release of large amount of the absorbed energy.

While fitting the LIG signals, the coefficients M_i and M_f were normalized to M_e, which was set equal to 1. In all samples under study, the electrostrictive and instantaneous thermal contributions have the sign opposite to that obtained for the fast thermal contribution. The fast energy redistribution is characterized by a few nanoseconds time constant: $\tau_f \approx 4$ ns in [EMIm][$EtSO_4$] and $\tau_f \approx 1$ ns in C_3H_6O. In fact, in the present case of $\tau_f \leq \tau_L$ the instantaneous and fast energy redistribution processes become

Table 2. Parameters of the Investigated Liquids at 293 K

	ρ, kg/m^3	c_P, J/(mol K)	$v_s \times 10^{-3}$, m/s		β_s, GPa^{-1}	$\chi \times 10^8$, m^2/s		κ, W/(m K)	
[EMIm][EtSO$_4$]	1241 [a]	377 [b]	1.691 [f]	1.75 [s]	0.262 [s]	9.2 [l]	9.1 [s]	0.182 [j]	0.181 [s]
		388 [c]				9.0 [m]		0.186 [q]	0.186 [s]
		410 [p]				10.1 [i]			
C_3H_6O	791 [a]	125 [d]	1.193 [g]	1.17 [s]	0.918 [s]	9.5 [n]	10.3 [s]	0.162 [k]	0.176 [s]
	790 [o]	124 [o]	1.186 [h]			9.3 [o]		0.157 [o]	
			1.187 [o]						
Mixture	943 [a]	161 [e]		1.27 [s]	0.653 [s]	9.28 [r]	9.1 [s]		0.165 [s]

[a] The literature value is taken from ref 17. [b] The literature value is taken from ref 21. [c] The literature value is taken from ref 22. [d] The literature value, for 298.15 K, is taken from.23. [e] Estimated from the data of refs 21 and 23. [f] The literature value is taken from ref 24. [g] The literature value is calculated using v_s at 298 K and its temperature dependence coefficient from ref 25. [h] The literature value is calculated using v_s at 298 K [26] and its temperature dependence coefficient from ref 25. [i] The value has been determined at 303.08 K using dynamic light scattering.[27] [j] The literature value is taken from ref 28. [k] The literature value for 300 K is taken from ref 29 and recalculated for 293 K. [l] Calculated using data of *a*, *b*, and *j*. [m] Calculated using data of *a*, *c*, and *j*. [n] Calculated using data of *a*, *d*, and *k*. [o] The literature value is taken from ref 30 for 293.15 K and 1 bar. [p] The literature value is taken from ref 31. [q] The literature value is taken from ref 32. [r] For the binary mixture, the thermal diffusivity was predicted by the mass-weighted sum of the pure component data, for which values of 9.2×10^{-8} m^2/s and 9.3×10^{-8} m^2/s were used for [EMIM][EtSO$_4$] and acetone, respectively. [s] This work.

weakly distinguishable, so that the initial part of the signals, especially in C_3H_6O, may be reasonably well fitted using only fast thermal contribution with the appropriate amplitude $\tilde{M}_f$ and the effective $\tilde{\tau}_f$. As mentioned above, the laser excitation of molecules in the RTIL/acetone mixture is nonspecific and therefore the fast thermal contribution term was taken as a linear combination of the two similar terms with the time constants τ_f characteristic for pure substances.

The obtained values of fitted temporal parameters for all three samples and the calculated values of T_a are summarized in Table 1. The errors are estimated from the variations of the values defined from a few LIG signals.

3.3. Discussion. The values of the fitted parameters Ω_a and τ_{th} allow the sound speed and thermal diffusivity of the liquids to be calculated. Furthermore, by the combination of these directly accessible properties with literature data for density ρ and specific heat c_P, the isentropic compressibility and thermal conductivity can be derived. The sound speed (at 60.5 MHz in the RTIL, at 40.4 MHz in C_3H_6O, and at 43.9 MHz in their mixture) and the thermal diffusivity are derived considering the fringe spacing $\Lambda = 29.0 \pm 0.6$ μm. The literature data for ρ and c_P at 293 K and the results of our calculations are presented in Table 2. The corresponding values provided by independent measurements are also given for comparison.

The sound speed in acetone determined from the LIG signals agrees with the values taken from the literature within the error of our measurements (about 2%). A slightly larger discrepancy (about 3%) between measured and reported sound speed values in the RTIL may appear (see discussion in ref 8) due to the dispersion of the sound speed, which in this work was measured in the range of a few tens of megahertz. In the RTIL/C_3H_6O mixture, the speed of sound was found to be closer to that in pure C_3H_6O.

In the low-frequency limit the speed of sound is related to the isentropic compressibility $\beta_s = 1/\rho((\partial\rho)/(\partial P))$ as

$$v_s^2 = \frac{1}{\rho\beta_s} \quad (4)$$

The calculated values of β_s demonstrate how the addition of [EMIm][EtSO$_4$] to C_3H_6O reduces the compressibility of the mixture; in particular, with 14 mol % of [EMIm][EtSO$_4$] it becomes about 30% smaller.

The derived values are in reasonable agreement with the data known from the literature. This convinces in the applicability of the fitting model and illustrates the accuracy of our measurements accomplished using the LIGs technique. At present, the uncertainty is mainly defined by the 2% accuracy of fringe period determination. For the sake of completeness, it should be noted that this error can be further decreased by a factor of 4−5 (down to 0.1 μm) by means of a special calibration of the fringe spacing using a reference solution. Hence, the relative standard deviations of the sound speed values are estimated to become better than 2%, and those of the compressibility and the thermal diffusivity to decrease below 4%.

The value of the decay time of a LIG signal oscillations measured in the present experiment does not allow the viscosity, which primarily defines the acoustic wave decay constant, to be derived reliably. The experiment is characterized by the temporal resolution in the order of 1 ns and the pump pulse duration of 7 ns. Moreover, to enable measurements of high sound speeds the crossing angle of the pump beams is made small to provide larger fringe spacing of about 30 μm. In addition, the beams are focused. In this case, the decay time of the oscillations, which is determined by the finite diameter of the pump beams, appears to be significantly smaller in liquids under study than the acoustic wave decay time, which is, moreover, proportional to the square of the fringe spacing. Note in this context that even in ref 12, where just the unfocused beams have been employed, at the large (∼100 μm) fringe spacing the fitted values of the oscillations amplitude exponential decay parameter could not be directly related to viscosity of liquids under study. On the contrary, estimates show that at high sound speed values the observed decays of oscillations during 1.0−1.4 μs might rather correspond to a reasonable value of the pump beams spot diameter of ∼5 mm.

4. SUMMARY AND CONCLUSION

In conclusion, the nonlinear optical technique employing laser-induced gratings has been applied for the determination of thermophysical properties of the room temperature ionic liquid [EMIm][EtSO$_4$], acetone, and their binary mixture. For the first time to the best of our knowledge, the simultaneous measurements of thermal diffusivity and sound speed of RTILs

without seeding additives, which absorb pump radiation, has been successfully demonstrated.

The sound speed and thermal diffusivity of the liquid samples at ambient pressure and temperature 293 K have been derived from the LIG signals temporal profiles. In addition, isentropic compressibility and thermal conductivity have been determined. The technique showed high sensitivity to the variation of the mixture composition and reasonable accuracy in determination of the mentioned parameters of liquids. The good agreement of the evaluated values with those found in the literature and provided by alternative methods is convincing in both the accuracy of the technique and the applicability of the model employed for fitting the LIG signal temporal profiles.

The results obtained demonstrate the feasibility to apply the LIGs technique using 1064 nm radiation of broadly available Q-switched Nd:YAG lasers for systematic measurements of a number of parameters of ionic liquids or, in general, liquids or gases containing chemical species with CH_3-, CH_2-, or CH− groups. The technique appears to be a useful and convenient tool for determining a set of data necessary for modeling the properties of the ionic liquids with arbitrary composition, or for screening these liquids in the process of their tailor-making in accordance with the desired properties. Moreover, owing to the possibility to perform single-shot measurements, the LIGs technique can provide data at high repetition rates and hence may be employed for process monitoring and control purposes.

AUTHOR INFORMATION

Corresponding Author

*Phone: +44 (0)1224 272495. E-mail: j.kiefer@abdn.ac.uk.

ACKNOWLEDGMENT

Technical assistance of M. Cam, B. Roshani, and J. Lehmann is acknowledged. The authors are grateful to A. Douplik for providing access to the absorption spectrophotometer. Part of this work was supported financially by the German National Science Foundation (DFG), project SE 804/3-1, and by the Russian Foundation for Basic Research (RFBR), Grant 08-02-91958. The authors also acknowledge support from the Erlangen Graduate School in Advanced Optical Technologies (SAOT) and the priority program "Ionic Liquids", DFG-SPP 1191.

REFERENCES

(1) Welton, T. *Chem. Rev.* **1999**, *99*, 2071–2084.

(2) Freemantle, M. *Chem. Eng. News* **2000**, *78*, 37–50.

(3) *Ionic Liquids in Synthesis*; Wasserscheid, P., Welton, T., Eds.; Wiley-VCH: Mannheim, 2003.

(4) Holbrey, J. D.; Reichart, W. M.; Reddy, R. G.; Rogers, R. D. *Ionic Liquids as Green Solvents*; Seddon, K. R., Rogers, R. D., Eds.; ACS Symposium Series 856; American Chemical Society: Washington, DC, 2003.

(5) (a) Olivier-Bourbigou, H.; Magna, L.; Morvan, D. *Appl. Catal., A* **2010**, *373*, 1–56. (b) Roosen, C.; Muller, P.; Greiner, L. *Appl. Microbiol. Biotechnol.* **2008**, *81*, 607–614.

(6) (a) Plechkova, N. V.; Seddon, K. R. *Chem. Soc. Rev.* **2008**, *37*, 123–150. (b) Werner, S.; Haumann, M.; Wasserscheid, P. *Annu. Rev. Chem. Biomol. Eng.* **2010**, *1*, 203–230.

(7) (a) Lewandowski, A.; Swiderska-Mocek, A. *J. Power Sources* **2009**, *194*, 601–609. (b) Armand, M.; Endres, F.; MacFarlane, D. R.; Ohno, H.; Scrosati, B. *Nat. Mater.* **2009**, *8*, 621–629.

(8) (a) Noack, K.; Schulz, P. S.; Paape, N.; Kiefer, J.; Wasserscheid, P.; Leipertz, A. *Phys. Chem. Chem. Phys.* **2010**, *12*, 14153–14161. (b) Kiefer, J.; Pye, C. C. *J. Phys. Chem. A* **2010**, *114*, 6713–6720. (c) Dhumal, N. R.; Kim, H. J.; Kiefer, J. *J. Phys. Chem. A* **2009**, *113*, 10397–10404.

(9) Fröba, A. P.; Kremer, H.; Leipertz, A. *J. Phys. Chem. B* **2008**, *112*, 12420–12430.

(10) Eichler, H. J.; Günther, P.; Pohl, D. W. *Laser-Induced Dynamic Gratings*; Springer: Berlin, 1982.

(11) Wang, J.; Fiebig, M. *Int. J. Thermophys.* **1995**, *16*, 1353–1361.

(12) Frez, C.; Diebold, G. J.; Tran, C. D.; Yu, S. *J. Chem. Eng. Data* **2006**, *51*, 1250–1255.

(13) Demizu, M.; Terazima, M.; Kimura, Y. *Anal. Sci.* **2008**, *24*, 1329–34.

(14) Kiefer, J.; Fries, J.; Leipertz, A. *Appl. Spectrosc.* **2007**, *61*, 1306–1311.

(15) Dhumal, N. R.; Kim, H. J.; Kiefer, J. *J. Phys. Chem. A* **2011**, *115*, 3551–3558.

(16) (a) Kiefer, J.; Kozlov, D. N.; Seeger, T.; Leipertz, A. *J. Raman Spectrosc.* **2008**, *39*, 711–721. (b) Seeger, T.; Kiefer, J.; Weikl, M. C.; Leipertz, A.; Kozlov, D. N. *Opt. Express* **2006**, *14*, 12994–13000.

(17) Lehmann, J.; Rausch, M. H.; Leipertz, A.; Froeba, A. P. *J. Chem. Eng. Data* **2010**, *55*, 4068–4074.

(18) Eichler, H.; Salje, G.; Stahl, H. *J. Appl. Phys.* **1973**, *44*, 5383–5388.

(19) Boyd, R. W. *Nonlinear Optics*, 2nd ed.; Academic Press: New York, 2003.

(20) Hubschmid, W.; Hemmerling, B.; Stampanoni-Panariello, A. *J. Opt. Soc. Am. B* **1995**, *12*, 1850–1854.

(21) Zhang, Z.-H.; Tan, Z.-C.; Sun, L.-X.; Jia-Zhen, Y.; Lv, X.-C.; Shi, Q. *Thermochim. Acta* **2006**, *447*, 141–146.

(22) Ge, R.; Hardacre, C.; Jacquemin, J.; Nancarrow, P.; Rooney, D. W. *J. Chem. Eng. Data* **2008**, *53*, 2148–2153.

(23) Malhotra, R.; Woolf, L. A. *J. Chem. Thermodynam.* **1991**, *23*, 867–876.

(24) Gomez, E.; Gonzalez, B.; Calvar, N.; Tojo, E.; Dominguez, A. *J. Chem. Eng. Data* **2006**, *51*, 2096–2102.

(25) http://www.kayelaby.npl.co.uk/general_physics/2_4/2_4_1.html (accessed April 18, 2011).

(26) Acosta, J.; Arce, A.; Rodil, E.; Soto, A. *J. Chem. Eng. Data* **2001**, *46*, 1176–1180.

(27) For pure [EMIM][$EtSO_4$], the thermal diffusivity and sound speed was determined to be 10.05 m^2/s at 303.08 K and 1699.37 m/s 298.06 K using dynamic light scattering (DLS). While for the measurement of sound speed by DLS an uncertainty of less than 0.5% can be guaranteed for ILs, their thermal diffusivity could only be determined with relatively large uncertainties of about 5%. See Fröba, A. P.; Leipertz, A. *Characterization of Ionic Liquids and Their Mixtures with Co-Solvents by Dynamic Light Scattering (DLS)*; Proc. 9th Asian Thermophysical Properties Conference, Beijing, China, 2010.

(28) Ge, R.; Hardacre, C.; Nancarrow, P.; Rooney, D. W. *J. Chem. Eng. Data* **2007**, *52*, 1819–1823.

(29) Vargaftik, N. B.; Vinogradov, Yu. K.; Yargin, V. S. *Handbook of Physical Properties of Liquids and Gases: Pure Substances and Mixtures*; Begell House: New York, 1996.

(30) Lemmon, E. W.; Huber, M. L.; McLinden, M. O. *NIST Standard Reference Database 23: Reference Fluid Thermodynamic and Transport Properties — REFPROP*, Version 9.0; National Institute of Standards and Technology, Standard Reference Data Program: Gaithersburg, Maryland, 2010.

(31) Fernandez, A.; Torrecilla, J. S.; Garcia, J.; Rodriguez, F. *J. Chem. Eng. Data* **2007**, *52*, 1979–1983.

(32) Fröba, A. P.; Rausch, M. H.; Krzeminski, K.; Leipertz, A. *Int. J. Thermophys.* **2010**, *31*, 2059–2077.